RSC Advances

ROYAL SOCIETY OF CHEMISTRY

www.rsc.org/advances
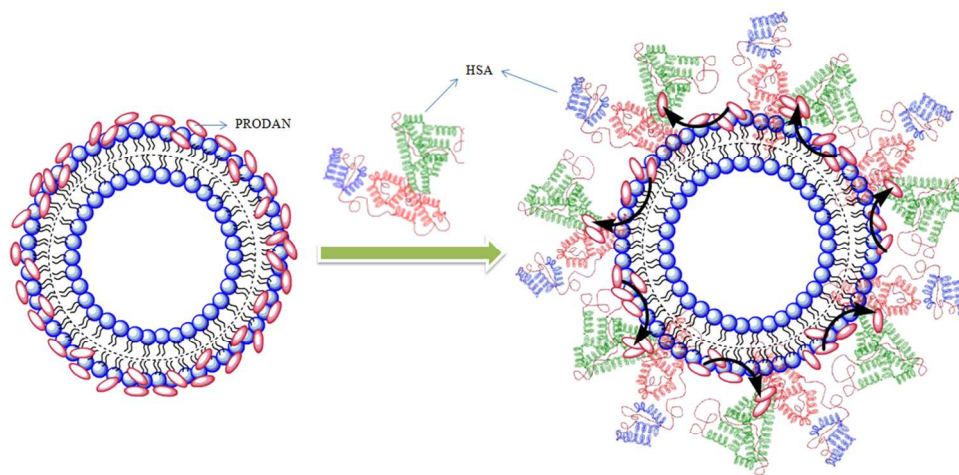
428x237mm (72 x 72 DPI)

1   **Interaction of Human Serum Albumin with Liposomes of Saturated and Unsaturated**

2   **Lipids of Different Phase Transition Temperatures: A Spectroscopic Investigation by**

3   **Membrane Probe PRODAN**

4

5   **Raina Thakur,[a] Anupam Das[a] and Anjan Chakraborty[a*]**

6   **[a]Department of Chemistry,**

7   **Indian Institute of Technology Indore, Madhya Pradesh, India.**

8

9

10

11

12

13

14   <u>**Author to correspondence:**</u>

15   Dr. Anjan Chakraborty

16   Email: anjan@iiti.ac.in

17   Fax: +91(0)731-2366382

18   Tel: +91(0)731-2438706

19

20

21

22

23

24

25   **Abstract.**

26   The interaction of Human serum albumin (HSA) with liposomes made of saturated and

27   unsaturated phosphocholines having distinctly different phase transition temperature has been

28   studied using circular dichroism (CD), steady state and time resolved fluorescence spectroscopic

29   techniques. We used *1,2-dipalmitoyl-sn-glycero-3-phosphocholine* (DPPC), *1,2-dimyristoyl-sn-*

30   *glycero-3-phosphocholine* (DMPC) as saturated lipids and *1,2-dioleoyl-sn-glycero-3-*

31   *phosphocholine* (DOPC), *2-oleoyl-1-palmitoyl-sn-glycero-3-phosphocholine* (POPC) as

32   unsaturated lipids to prepare liposomes. The CD measurement reveals that the liposomes induce

33   some kind of stabilization in HSA. The steady state and time resolved fluorescence spectra of

34   PRODAN (6-propionyl 1-2-dimethylaminonaphthalene) was monitored to unravel the interaction

35   between liposome and HSA. We observed that HSA partially penetrates in the liposomes due to

36   hydrophobic interaction and destabilizes the packing order of lipid bilayer leading to leakage of

37   the probe molecules from the liposome. It was found that HSA preferably penetrates into the

38   liposomes, which are less prehydrated at room temperature. Thus penetration is higher in DPPC

39   and DMPC liposomes as these liposomes are less prehydrated due to higher phase temperature

40   (43^0 C and 23 ^{0} C respectively). On the other hand HSA has less penetration in DOPC and

41   POPC liposomes because these liposomes are more hydrated owing to lower phase transition

42   temperature (-20 ^{0} C and -2 ^{0} C respectively). The time resolved fluorescence measurements

43   revealed that penetration of HSA into liposomes brings in release of PRODAN molecules.

44   Incorporation of HSA in all the liposomes results in significant increase in the rotational

45   relaxation time of PRODAN. This fact confirms that HSA penetrates into the liposome and

46   forms bigger complex.

47

48   **Key Words:** PRODAN, Liposomes, Hydration, HSA, Penetration,

49

50

51

52

53 **1. Introduction.**

54 Plasma membrane is a complicated assembly of lipids and proteins, organized into various
55 specialized microdomains with versatile diversity.[1] To overcome the problems associated with
56 this diversity it is worthwhile to use synthetic liposomes or vesicles which mimic the geometry
57 and topology of cell membranes.[2] Phospholipids form the fundamental matrix of natural
58 membranes and represent the environment in which many proteins and various macro molecules
59 display their activity.[3] Therefore characterization of lipid membranes with sufficient selectivity
60 will help to study the variation around its bulk properties.[4] Owing to their small size, amphiphilic
61 character, and biocompatibility, liposomes or vesicles are promising systems for drug delivery
62 through the blood stream.[5] Therefore it is necessary to visualize the stability of liposomes in
63 presence of serum proteins.[6] Human Serum Albumin (HSA) is the most prominent component of
64 blood plasma. It serves as transport protein for several endogenous and exogenous ligands as
65 well as for various drug molecules.[7-8] HSA also binds well with fatty acids.[9] It is reported that
66 proteins partially penetrate and deform the lipid bi-layer.[10] HSA penetrates into the vesicle and
67 gets adsorbed on the surface of vesicles to some extent. Packing of hydrophobic tails of the lipid
68 is also disturbed in presence of HSA.[11] Charbonneau et al. suggested that both hydrophobic and
69 hydrophilic interactions occur for liposome-HSA systems.[12] Various groups suggested that for
70 prolonged circulation of liposomes in blood stream and to provide stability, cholesterol should be
71 incorporated in the vesicle.[13]

72 Although there are a few reports regarding liposome-HSA system,[10-12] however, none of the
73 studies addressed the nature of interaction between liposome and HSA by fluorescence
74 spectroscopy using a polarity sensitive membrane probe. Moreover, it was not answered what
75 will be fate of encapsulated molecules inside the liposome upon interaction with HSA.
76 Therefore, it is desirable to undertake a study which involves different kind of liposomes. The
77 present work has the novelty because it involves four different phosphatidylcholines lipids with
78 zwitterionic head groups. These lipids are widely different in terms of their phase transition
79 temperature and nature of their acyl chain. *1,2-dipalmitoyl-sn-glycero-3-phosphocholine* (DPPC)
80 *and 1,2-dimyristoyl-sn-glycero-3-phosphocholine* (DMPC) are saturated phospholipids while
81 *1,2-dioleoyl-sn-glycero-3-phosphocholine* (DOPC) and *2-oleoyl-1-palmitoyl-sn-glycero-3-*
82 *phosphocholine* (POPC) contain unsaturation in their acyl chain (Scheme1).

3

83   Phosphatidylcholines are dominant in eukaryotic membranes.[14] The lipids of more metabolically

84   active membranes are considerably more unsaturated. POPC bilayers provide relevant models for

85   the matrix of the endoplasmic reticulum.[15] DPPC exhibits properties very similar to those of

86   sphingomyelin which is the most abundant lipid in plasma membrane.[16] In our previous studies,

87   we encapsulated anticancer drug ellipticine in DPPC vesicles and studied its release by various

88   bile salts.[17] The present study is done to reveal protein-liposome interaction and the transport of

89   various drugs through lipid bilayers via Human Serum Albumin (HSA) to the target site with the

90   help of fluorescence spectroscopy. Fluorescence spectroscopy has several advantages including

91   a high sensitivity, a noninvasive nature, an intrinsic time scale and an excellent response to the

92   physical properties of membrane.[18] For this purpose PRODAN (Scheme 1) has been chosen as a

93   probe molecule primarily to study the environment inside the liposomes and to reveal the

94   liposome-HSA interaction. PRODAN is very sensitive towards environmental polarity and the

95   origin of its solvatochromatic nature have been debated.[19] It shows large spectral shifts when

96   attached to membranes.[20] The sensitivity of emission properties of PRODAN towards polarity is

97   attributed to a large difference between the dipole moments in its ground (S_0) and excited (S_1)

98   states.[21] According to various calculations, difference in dipole moment of PRODAN from 5.50

99   to 10.20 D causes a shift in the $S_0 \rightarrow S_1$ transition.[22a] Recently Samanta and co-workers[22b] have

100   suggested this value to be 4.40 to 5.0 D based on transient dielectric loss measurements. In

101   PRODAN, both locally excited (LE) and twisted internal charge transfer (TICT) states

102   simultaneously exist.[23] This amazing feature of PRODAN makes it a useful probe to study

103   structure, function and dynamics of proteins and membranes.[20,24] The probe has widely been

104   used to study the dynamics inside a reverse micelles.[25] It was reported that in aqueous reverse

105   micelle PRODAN molecules are distributed in three regions according to the polarity of that

106   particular region.[25] PRODAN, having higher water solubility is loosely anchored to the

107   bilayer.[26] Hof and co-workers studied solvent relaxation of various probes including PRODAN

108   in phosphocholine vesicles.[27] The emission maximum of PRODAN depends upon the phase state

109   of phospholipids. It usually emits at 440 nm in gel and at 490 nm in liquid crystalline phase. The

110   shift in emission band from gel to liquid crystalline phase takes place due to dipolar relaxation in

111   liquid crystalline phase of phospholipid but not in gel phase. This dipolar relaxation originates

112   due to a few water molecules present in bilayer at the glycerol backbone where fluorescence

113   moiety of PRODAN actually resides.[28] The complex character of emission peak of PRODAN in

114   the lipid bilayer can be explained assuming that both twisted and planar configuration emit in the

115   bilayer.[27c] As emission of PRODAN is highly sensitive, it has been used to study different

116   protein molecules. Chattopadhyay et al. have reported the red edge excitation spectra (REES) of

117   PRODAN in different proteins like spectrins.[29]   Hydration dynamics studies of HSA using

118   PRODAN as probe reveals that hydration level of different domains is different and they have

119   different time scales for hydration.[30] HSA contains only one tryptophan residue at position 214

120   (Trp214) in domain II and one free cystine residue at position 34 in domain I, moreover it has 17

121   disulphide bonds.[31] The free thiol group allows site specific labeling of protein with

122   chromophoric or fluorescent probes.[32] PRODAN binds with HSA within Sudlow site I i.e. on

123   warfarin binding site.[33] So far, interaction of PRODAN with liposome and HSA is reported

124   individually. But interaction of HSA and liposome is still unexplored using a membrane probe.

125   Therefore, photophysics of PRODAN by steady state and time resolved spectroscopy will not

126   only be able to reveal the environment inside the HSA, liposome and liposome-HSA complex

127   but will also give a new insight regarding the interaction between liposomes and HSA. This

128   study may further help in designing a novel drug delivery system for various drugs exhibiting

129   properties very similar to PRODAN.

130

131

132

133

134

135

136

137

138

139

5

140

141

142

143

144

DPPC

DMPC

145

146

147

148

149

DOPC

POPC

150

151

152

153
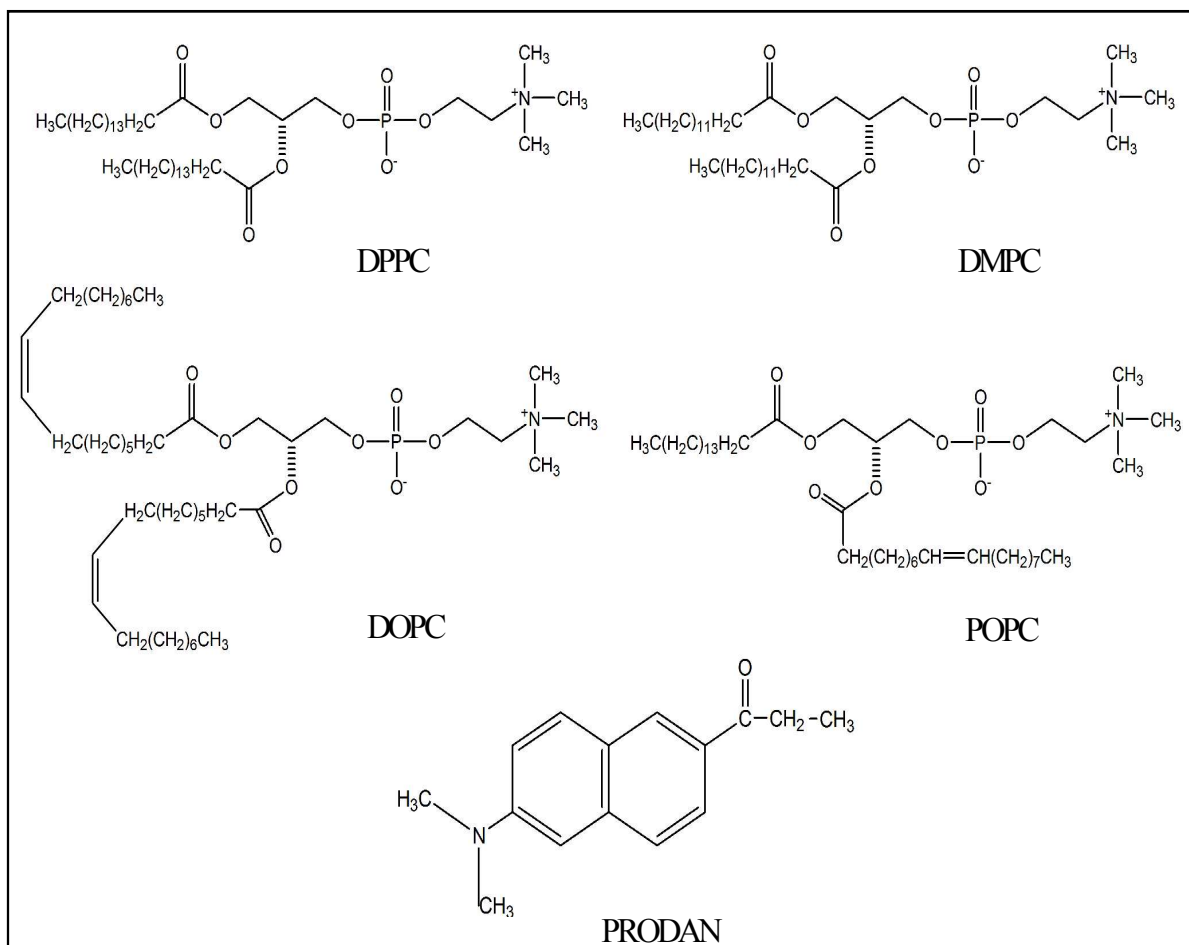
PRODAN

154   **Scheme 1**

155

156

157

158

159

160

6

161   **2. Experimental Section.**

162   **2.1. Materials.** PRODAN, HSA, urea and all the lipids (DPPC, DMPC, POPC and DOPC)

163   were purchased from Sigma-Aldrich. Na_2HPO_4 and NaH_2PO_4 were purchased from Merck.

164   All the chemicals were used without further purification. All the experiments were performed

165   in Milli Q water. Stock solution of PRODAN was prepared in methanol. Required amount of

166   methanolic solution was taken in a volumetric flask and dried under vacuum to create a thin

167   film of PRODAN. An appropriate amount of phosphate buffer (25 mM) was added to it and

168   was sonicated for two hours. Small Unilamellar Vesicles (SUV) were prepared by ethanol

169   injection method as described earlier.[17] The stock solution of lipid was prepared in ethanol.

170   The desired amount of ethanolic lipid solution was rapidly injected into the aqueous

171   solution of PRODAN (above the phase transition temperature of respective lipids) and

172   was equilibrated for 60 minutes. The concentration of lipid in the solution was 0.4 mM and

173   the percentage of ethanol was less than 1% (v/v). The molar ratio of PRODAN to lipid was

174   around 1:200. Required amount of HSA was added to the solution of SUV to prepare stock

175   solution of HSA and Lipid. This solution was incubated for 30 minutes before the

176   measurements

177   **2.2. Spectroscopic Measurements.** Steady state absorption spectra were taken in a Varian

178   UV-Vis spectrometer (Model: Cary 100). Emission spectra were taken in a Fluoromax-4p

179   fluorimeter from Horiba Jobin Yovon (Model: FM-100). The samples were excited at 375

180   nm. The fluorescence spectra were corrected for the spectral sensitivity of the instrument.

181   The excitation and emission slits were 2/2 nm for the emission measurements. All the

182   measurements were done at 25º C.

183   For the time resolved studies, we used a picosecond time correlated single photon counting

184   (TCSPC) system from IBH (Model: Fluorocube-01-NL). The experimental setup for TCSPC

185   has been described elsewhere.[34] The samples were excited at 375 nm using a picosecond

186   diode laser (Model: PicoBrite-375L). The repetition rate was 5 MHz. The signals were

187   collected at magic angle (54.70º) polarization using a photomultiplier tube (TBX-07C) as

188   detector which has a dark counts less than 20 cps. The instrument response function of our

189   setup is ~140 ps. The data analysis was done using IBH DAS (version 6) decay analysis

190   software. The fluorescence decay was described as a sum of exponential functions:

191
$$D(t) = \sum_{i=1}^{n} a_i \exp\left(\frac{-t}{\tau_i}\right)$$
(1)

192   where $D(t)$ is the normalized fluorescence decay and τ_i are the fluorescence lifetimes of various

193   fluorescent components and a_i are the normalized pre-exponential factors. The amplitude

194   weighted lifetime is given by:

195
$$\langle \tau \rangle = \sum_{i=1}^{n} a_i \tau_i$$
(2)

196   The quality of the fit was judged by reduced Chi square (χ^2) values and the corresponding

197   residual distribution. To obtain the best fitting in all of the cases, χ^2 was kept near to unity. The

198   same setup was used for anisotropy measurements. For the anisotropy decays, we used a

199   motorized polarizer in the emission side. The emission intensities at parallel and perpendicular

200   polarizations were collected alternatively until a certain peak difference between parallel (II) and

201   perpendicular ($\perp$) decay was achieved. The same software was also used to analyze the

202   anisotropy data. The time resolved anisotropy was described with the following equation:

203
$$r(t) = r_0 \left[\beta_{fast} \exp\left(-\frac{t}{\phi_{fast}}\right) + \beta_{slow} \exp\left(-\frac{t}{\phi_{slow}}\right) \right]$$
(3)

204   where $r(t)$ is the rotational relaxation correlation function and r_0 is the limiting anisotropy and

205   ϕ_{fast} and ϕ_{slow} are the individual rotational relaxation time and β_{fast} and β_{slow} are the amplitudes

206   of rotational relaxation time.

207   **2.3. Circular Dichroism (CD).** CD is a sensitive technique to monitor the conformational

208   changes in proteins. CD spectra of HSA and its lipid complexes were recorded with a Jasco J-

209   815 spectrometer (Jasco, Tokyo, Japan). For measurements in the far UV region (200-270), a

210   quartz cell with a path length of 0.1 cm (Hellma, Muellheim/Baden, Germany) was used in

211   nitrogen atmosphere. The HSA concentration was kept constant (10μm) while varying lipid

212   concentration (0.1 mM, 0.3 mM and 0.6 mM). An accumulation of five scans with a scan speed

213   of 20 nm/min was performed data were collected for each sample from 200 to 270 nm. The

214   sample temperature was maintained at 25ºC using Escy temperature controller circulating water

215   bath connected to the water-jacketed quartz cuvettes. Spectra were corrected for buffer signal.

3. Results and Discussion.

3.1. Interaction of PRODAN with HSA.

218   PRODAN exhibits emission maxima at 520 nm in aqueous buffer solution. Addition of HSA

219   to the buffer solution of PRODAN diminishes the intensity at 520 nm and additionally a band

220   appears at 455 nm. The band at 455 nm is attributed to the LE state of HSA bound

221   PRODAN. The appearance of LE state indicates that PRODAN experiences a less polar

222   environment in HSA. With increase in HSA concentration, the contribution of TICT band

223   decreases while that of LE band increases which implies that more number of PRODAN

224   molecules bind with HSA. Interestingly, we obtained an isoemissive point at around 510 nm

225   which implies that there are two emitting species in the excited state. The emission spectrum

226   of PRODAN in presence of 20 µM of HSA was deconvoluted by a combination of the

227   lognormal functions to show simultaneous existence of CT and LE species (Figure 1A) by

228   taking the emission spectrum of PRODAN in aqueous buffer solution as reference. We

229   estimated binding constant of PRODAN molecules with HSA using Bensei-Hidlebrand

230   equation for 1:1 complex as following.

231   $$I_f = \frac{I_f^0 + I_{PROD-HSA}k_1[HSA]}{1 + k_1[HSA]} \qquad (4)$$

232   where, I_f^0 is the fluorescence intensity of PRODAN in absence of HSA and $I_{PROD-HSA}$ is the

233   fluorescence intensity when all PRODAN molecules form complex with HSA. The nonlinear

234   regression analysis following equation 4 yields the binding constant (k_1) around 7×10^5 M^{-1}

235   (Figure 1B). The earlier report [29a] states that PRODAN binds with HSA at Sudlow site I i.e.

236   on warfarin binding site. This observation is consistent with our experimental result (The

237   data are not shown). The formation of complex between PRODAN and HSA is exothermic

238   with value of ΔHº = -22.82 KJ mol^{-1}.[33] It was also reported that PRODAN does not bring

239   about any conformational changes in HSA.[29a]

240
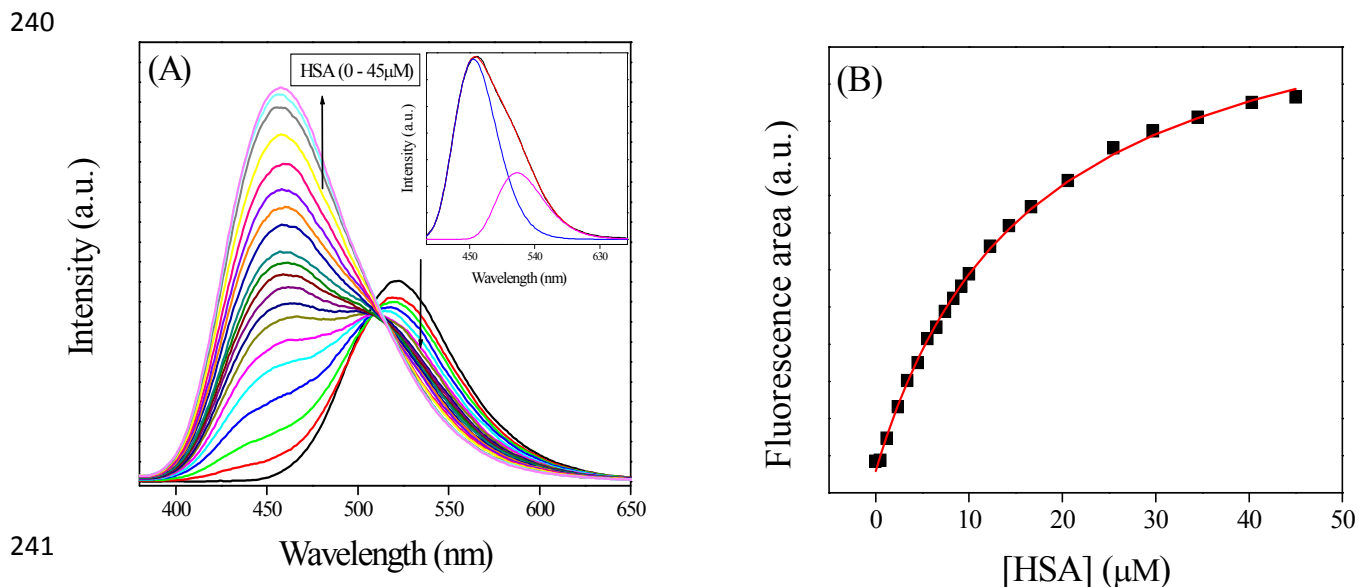
241

242 **Figure 1.** (A) The emission spectra of PRODAN at different concentration of HSA. Inset is
243 the emission spectrum of PRODAN in presence of 20 µM HSA that has been deconvoluted
244 in LE and TICT state. (B) The fitted binding curve between PRODAN and HSA following
245 equation 4.

246 To gain more specific local information about the binding of PRODAN to HSA, we
247 estimated the energy transfer efficiency between PRODAN and HSA by monitoring the
248 emission spectra of Trp214 of HSA (Figure 2). The distance between Trp214 and PRODAN
249 was estimated from the energy transfer efficiency expression:

250 $$E = 1 - \frac{I}{I_0} = \left(1 + \frac{R^6}{R_0{}^6}\right)^{-1} \tag{5}$$

251 where I_0 and I are the intensities of Trp214 emission measured for the protein alone and for
252 PRODAN-HSA complex, respectively. Figure 2 reveals that the efficiency of energy transfer
253 between Trp214 of HSA and PRODAN is around 43%. Such weak energy transfer indicates that
254 PRODAN molecules bind at a location which is away from tryptophan. In the equality, R is the
255 distance between Trp214 and PRODAN in Angstrom. R_0 is a characteristic Forster distance for
256 50% energy transfer efficiency related to the properties of donor and acceptor, and can be
257 calculated using following equation

10

258     $$R_0^{\ 6} = 8.79 \times 10^{-5} n^{-4} \kappa^2 \phi_0 \int \varepsilon(\lambda) f(\lambda) \lambda^4 d\lambda \Big/ \int f(\lambda)$$ (6)

259   where, n is the refractive index of the medium, κ^2 is a geometric factor related to the relative

260   orientation of the transition dipole moments of the donor and acceptor, $\varepsilon(\lambda)$ is the molar

261   absorptivity of PRODAN, and $f(\lambda)$ is the normalized fluorescence intensity of Trp214.

262   Therefore, R_0 is calculated from equation 6 using geometrical parameter κ^2 as 2/3. These

263   parameters yielded a value for R_0 of 26 Å, leading to an estimate for R, the apparent distance

264   between Trp214 and PRODAN being 24 Å. We fitted the quenching data with a modified

265   Stern-Volmer equation as follows:

266     $$\frac{I_0}{I} = \frac{1 + K_{SV}[Q]_L}{(1 + K_{SV}[Q]_L)(1 - f_B) + f_B}$$ (7)

267   In this equation I_0 is the intensity of HSA in absence of PRODAN. K_{SV} is the Stern-Volmer

268   quenching constant and

269     $$f_B = \frac{I_{0,B}}{I_0}$$ (8)

270   where $I_{0,B}$ is fluorescence intensity of the tryptophan accessible to quencher. Thus the

271   estimated K_{SV} and f_B were around 1.77×10^6 M^{-1} and 0.54 respectively.

272

273

274

275

276

277

278

11
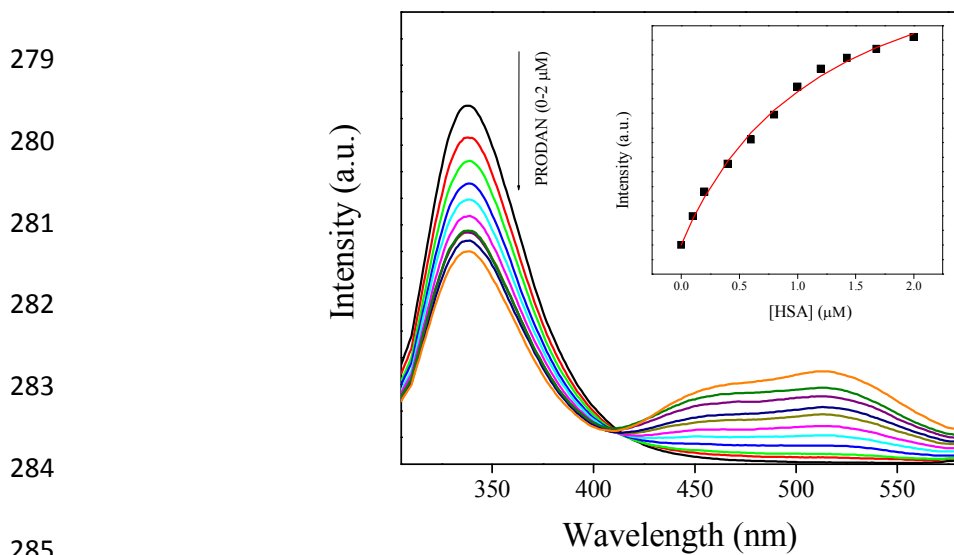
Figure 2. Emission spectra of HSA (10 μM) in presence of different concentration of PRODAN (0-2 μM).

We measured the fluorescence lifetime of PRODAN at 457 and 520 nm at different concentration of HSA (Table S_1 in the supporting information). In presence of 1 μM HSA, PRODAN exhibits the lifetime components around 0.73 ns (55%) and 3.60 ns (45%) at 457 nm. The decay at 50 μM concentration of HSA at the same wavelength is comprised of 0.90 ns (33%) and 4.00 ns (67%) components with an average lifetime of 3.00 ns. We assign the species with time component of 4.00 ns to HSA bound PRODAN and the species with time component of 0.90 ns to the free PRODAN species in aqueous medium. Our result is consistent with the measurement made by Basak and co-workers.[29b] The increase in fluorescent quantum yield and lifetime of PRODAN and its derivative when bound to protein is due to reduced conformational freedom of the amine and carbonyl groups because of the close packing of surrounding protein.[30] The significant increase in longer component from 45% to 67% upon addition of 50 μm HSA clearly indicates that PRODAN molecules are entrapped inside the hydrophobic pocket of HSA. Table S_1 reveals a similar component at 520 nm when PRODAN binds with HSA. The lifetime at 520 nm was fitted with a bi-exponential function. The increase in nanosecond component which represents HSA bound PRODAN species from 26% to 45% confirms the binding of PRODAN molecules with HSA.

3.2. Interaction of PRODAN with Liposomes. In this section we first encapsulate PRODAN in different liposomes. Addition of liposomes to aqueous solution of PRODAN causes a blue shift in emission spectra followed by a new band at 435 nm. This band is assigned as LE state of PRODAN. The appearance of LE band indicates that PRODAN molecules are encapsulated inside the liposomes. Interestingly, we observe an isoemissive point in DPPC and DMPC liposomes which indicates the existence of two emissive species in these two liposomes (Figure 3).
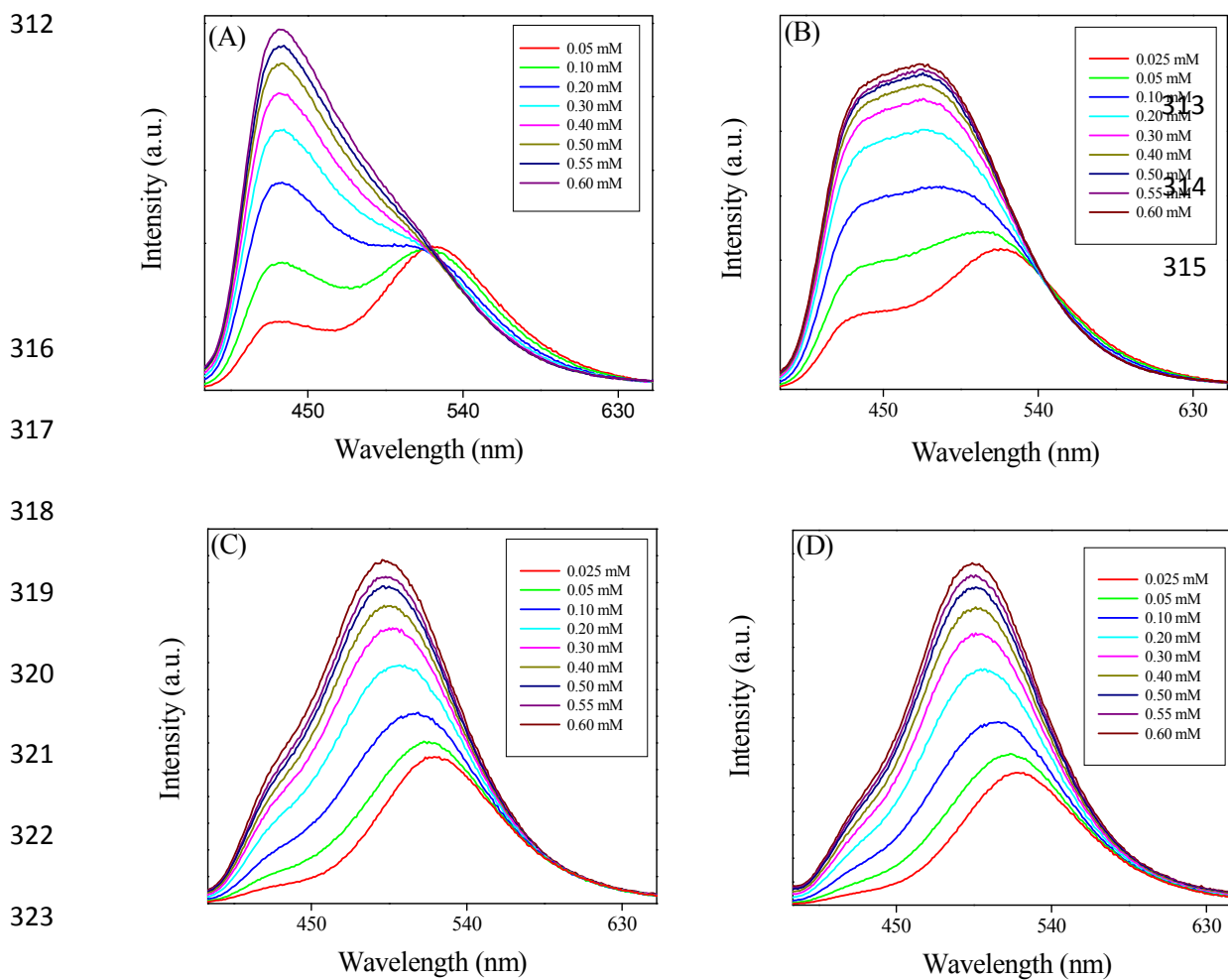
Figure 3. The emission spectra of PRODAN at different concentration of liposomes (A) DPPC (B) DMPC (C) DOPC and (D) POPC liposomes.

328   On the other hand isoemissive point was not observed when PRODAN is incorporated into

329   DOPC and POPC liposomes. A similar observation was reported by Correa and co-workers

330   in case of DOPC liposomes.[35] They explained this observation with the model proposed by

331   Chong and co-workers.[26a] The lack of isoemissive point in POPC and DOPC liposomes may

332   be due to absence of a prominent LE state in DOPC and POPC liposomes. To explain this

333   observation we consider the differences in the hydration level of liposomes which further

334   depends on their phase transition temperature. DPPC and DMPC have phase transition

335   temperatures around $43^{\circ}C$ and $23^{\circ}C$ respectively while POPC and DOPC have phase

336   transition temperature around - $2^{\circ}C$ and - $20^{\circ}C$ respectively. It is reported by Horta and co-

337   workers[36] that the liposomes having lower phase transition temperature is more hydrated than

338   liposomes having higher phase transition temperature. Again because of much lower phase

339   transition temperature, DOPC and POPC are significantly much more hydrated and are much

340   softer than DPPC and DMPC at room temperature. PRODAN molecules are mostly

341   encapsulated in the interfacial region of DOPC and POPC. Since DOPC and POPC exist in

342   the liquid crystalline phase at room temperature, the non polar region is less motionally

343   restricted compared to that in interfacial region. Thus lack of a prominent LE state may be

344   responsible for absence of an isoemissive point.

345   The normalized emission spectra of PRODAN (Figure 4) in different liposomes reveal that

346   maximum blue shift takes place in DPPC liposomes. This fact also indicates that DPPC and

347   DMPC are more hydrophobic as compared to DOPC and POPC due to their higher phase

348   transition temperature and due to difference in their prehydration levels. Correa and co-

349   workers correlated the maximum emission band energy of PRODAN ($E_{em\text{-}PRODAN}$) with

350    $E_{T(30)}$ polarity scale for different solvents by the following equation.[35]

$$E_{T(30)} = 147 \pm 5 - (1.62 \pm .02) E_{em-PRODAN} \qquad \text{351}$$
$$n = 23, r = 0.98$$

(9)

352

353   Following this equation $E_{T(30)}$ values as obtained for DPPC, DMPC, POPC and DOPC

354   liposomes are 41.7, 47, 52 and 54 Kcal/mol respectively. The different micropolarity as

355   experienced by PRODAN in different liposomes could be attributed to the difference in their

356   prehydration levels which further depends on phase transition temperatures.

14

357

358

359

360

361

362

363

364
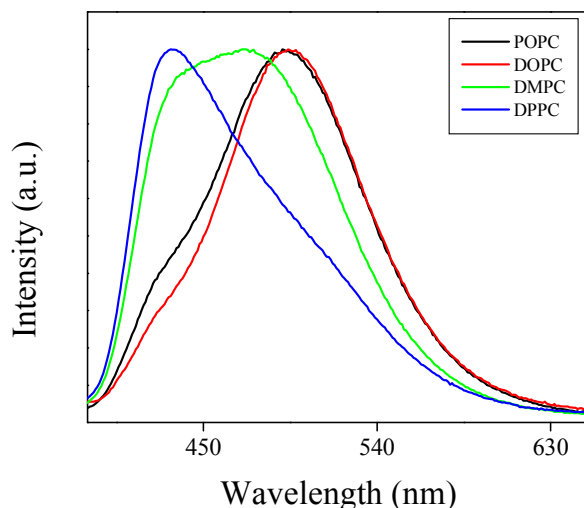
365 **Figure 4.** Normalized emission spectra of PRODAN in different liposomes.

366 At room temperature DPPC vesicles remain in sol gel phase (SG) and DMPC vesicles remain

367 in nearly liquid crystalline (LC) phase. As, torsion of the $-N(CH_3)_2$ are more restricted in SG

368 phase of the phospholipid bilayer than that in LC phase, LE band has less contribution in LC

369 phase compared to that in sol gel phase. DOPC and POPC liposomes exist completely in LC

370 phase at room temperature. Thus they have similar emission spectra for PRODAN at room

371 temperature which is clear from Figure 4. We estimated the partition coefficient of prodan in

372 different liposomes using the following equation[37]

373 $$\frac{1}{F} = \frac{55.6}{\left(K_P F_0 L\right)} + \frac{1}{F_0}$$ (10)

374

375 where F_0 and F are fluorescence intensities of PRODAN molecules in aqueous and in

376 lipid phase, respectively, L is the lipid concentration and the molar concentration of water

377 was considered to be 55.6 M. Thus using equation 10 and the slopes from Figure 5, the

378 calculated K_P values are 1.0×10^5, 5.8×10^5, 2.8×10^5, 2.6×10^5 for DPPC, DMPC, POPC

379 and DOPC liposomes respectively. Notably the lower partition coefficient in DPPC

380 liposomes compared to that in other liposomes stems from the fact that the interfacial region

381   of DPPC is much more rigid due to its sol gel phase and this rigidity hinders the

382   encapsulation of more number of PRODAN molecules. The liposomes like DMPC, DOPC

383   and POPC remain in liquid crystalline phase at room temperature and they allow PRODAN

384   to penetrate in the interfacial region.

385

386

387

388

389

390

391
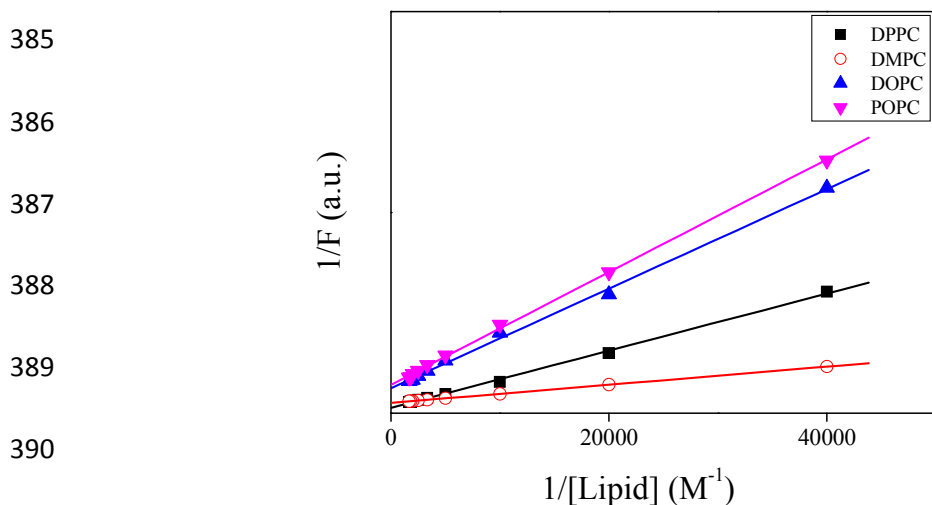
392   **Figure 5.** Double reciprocal plot of the intensity of PRODAN with respect to concentration

393   different liposomes.

394   We estimated the lifetime of PRODAN at various concentrations of liposomes at 440 and

395   520 nm. The values of lifetime for different vesicles are summarized in Table S_2A and Table

396   S_2B (in supporting information) and the representative decays are shown in Figure 6.

397   PRODAN exhibits a bi-exponential decay in aqueous buffer solution at 520 nm with the

398   lifetime components 0.62 ns (τ_1) and 1.8 ns (τ_2) with a population of 74% and 26%

399   respectively. Thus the average lifetime of PRODAN at 520 nm is around 0.93 ns. In DPPC

400   liposome, at 520 nm, where the emission spectra is predominantly from TICT state of

401   PRODAN has conspicuously dependence on the concentration of lipid and is well described

402   by a tri-exponential function. The picosecond component i.e. τ_1 remains same throughout the

403   concentration of DPPC and the nanosecond component i.e. τ_2 increased up to around 2.17 ns.

404   A third component of around 5.19 ns (τ_3) with a population of 31% appeared at higher

405   concentration of DPPC (Table S_2A). We, therefore, assign τ_1 component to the PRODAN

406   molecules remaining in the aqueous phase which drops from 74% to 53% upon increasing

407   the concentration of DPPC from 0 to 0.6 mM. The 2.17 ns component i.e. τ_2 may be ascribed

408   to the PRODAN molecules in aqueous phase or loosely bound in the interfacial region and

409   the longest component i.e. 5.20 ns (τ_3) component may come from the PRODAN molecules

410   strongly held inside the liposome. Interestingly, PRODAN at 435 nm in 0.6 mM DPPC

411   liposome where emission mainly comes from LE state exhibits a tri-exponential decay. The

412   components are 0.62 ns (17%), 2.73 ns (31%) and 6.57 ns (52%). We already assigned these

413   components to different locations in liposomes.

414   In DMPC liposome, the decays at 520 nm were fitted to a bi-exponential function with a

415   picosecond and a nanosecond component. As the liposome concentration increases and

416   incorporate more number of PRODAN molecules, the picosecond component disappeared

417   leading to a rise component around 1.65 ns (31%) and a nanoscecond component around 4.72

418   ns (69%). The decay proceeds with a rise component indicates that solvation takes place.

419   Surprisingly, in case of DPPC liposomes, we did not observe any rise component which

420   could be because of the fact that the aliphatic tail region of DPPC is more dehydrated than

421   that of DMPC. Table S_2B reveals that the decay of PRODAN in DMPC liposomes at 435 nm

422   is tri-exponential with picosecond component (τ_1) and two nanosecond components (τ_2 and

423   τ_3). The components are 0.74 ns (14%), 1.77 ns (31%) and 4.25 ns (55%). It is noteworthy

424   that τ_3 is significantly less in DMPC liposomes compared to that in DPPC liposomes. The

425   probable reason is that DMPC remains in nearly liquid crystalline phase at room temperature

426   while DPPC remains in sol-gel phase which brings in additional rigidity in DPPC compared

427   to that in DMPC. This may be responsible for higher time component in DPPC compared to

428   that in DMPC.

429

430

431

432

433

434
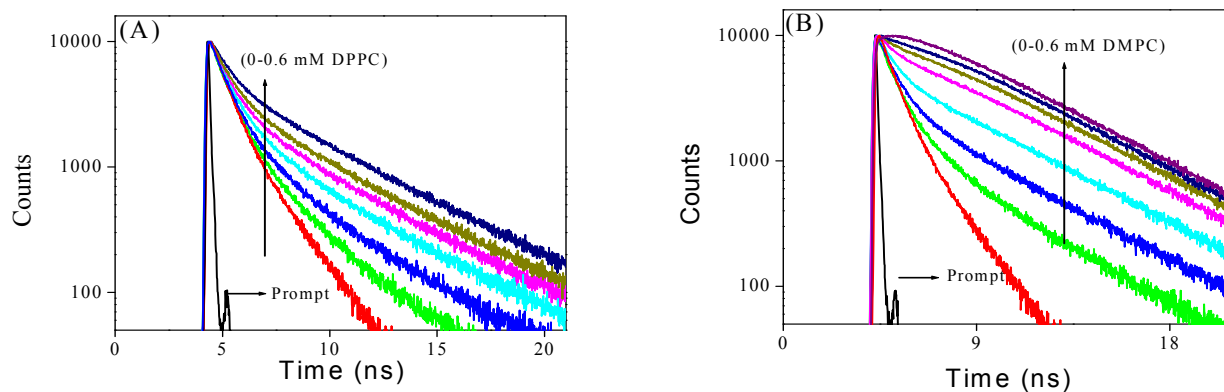
Figure 6. Decay of PRODAN at different concentration of liposomes (A) DPPC liposome
(B) DMPC liposome

In DOPC and POPC liposomes initially decay at 520 nm was bi-exponential with a picosecond component (~670 ps) originating from the PRODAN molecules in the aqueous phase and a nanosecond component around 2.65 to 2.69 ns. Due to low concentration of lipid two components are observed picosecond component in aqueous phase and the other nanosecond component in lipid phase. However, at higher concentration the decay becomes single exponential with time constant around 3.52 ns and 3.38 ns for DOPC and POPC liposomes respectively. These results are in accordance with that reported by Correa and co-workers.[35] At 435 nm the decays in DOPC and POPC were fitted to a biexponential function having a picosecond component around 0.840 ns and a nanosecond component around 2.60 to 2.70 ns. Notably, the longer components in POPC and DOPC liposomes at 520 and 435 nm are significantly smaller compared to longer component of DPPC and DMPC liposomes at the same wavelength. This observation may be explained by considering the fact that at room temperature both DOPC and POPC remain in liquid crystalline phase due to significant lower phase transition temperature compared to DPPC and DMPC. Therefore, PRODAN experiences a less constrained environment in DOPC and POPC liposomes giving rise to a shorter lifetime component as compared to DPPC and DMPC liposomes.

458

459

3.3. Interaction between liposomes and HSA.

3.3.1 CD Measurements. To gain a better insight on interaction of HSA with various liposomes CD measurements were performed using HSA, DPPC liposomes and POPC liposomes at various concentrations of these lipids. The CD spectra of HSA exhibit two negative minima at 208 and 217 nm, which is typical characterization of α-helix structure of proteins.[38a] Interaction between DPPC-HSA and POPC-HSA caused an increase in band intensity at all wavelengths of the far UV CD without any significant shift of the peaks (Figure 7). This indicates that both DPPC liposomes and POPC liposomes causes a slight increase in the α-helical structure of HSA. While heating HSA till 90°C and addition of 8M urea causes decrease in the band intensity at all the wavelengths (Figure7C). This signifies decrease in α-helical content upon denaturation of HSA.[38b] Thus we conclude that both the lipid upon interaction with HSA cause perturbation in the secondary structure of HSA but increase in α-helical content suggest that HSA is not denatured or unfolded during the interaction.[12]

Figure 7. CD spectra of (A) HSA and DPPC liposomes (B) HSA and POPC liposomes (C) Native HSA and denatured HSA.
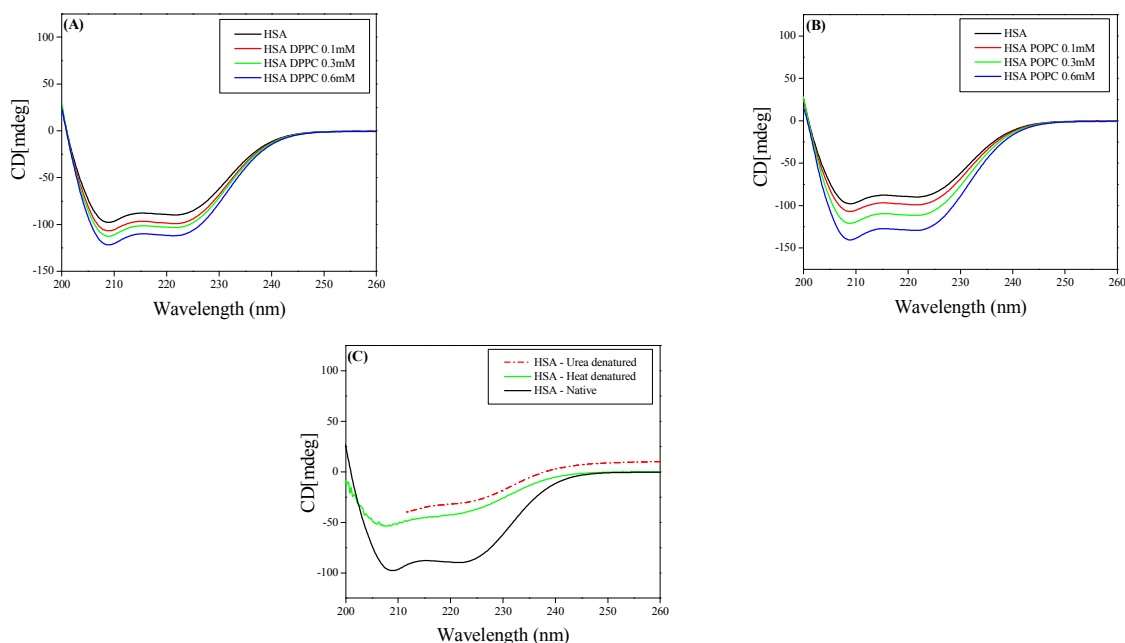
3.3.2. Steady state and Time resolved measurement.

Addition of HSA to PRODAN impregnated liposomes causes a quenching in the fluorescence
intensity of PRODAN. The continuous decrease in the intensity with addition of HSA to
PRODAN impregnated liposomes indicates that HSA interacts with the liposomes. Interestingly,
we observe a red shift in the emission spectra of PRODAN in DPPC liposomes (from 435 to 460
nm) while a blue shift is observed in DMPC (from 460 to 455 nm), DOPC (from 497 to 471 nm),
and POPC (from 490 to 467 nm) liposomes (Figure 8).
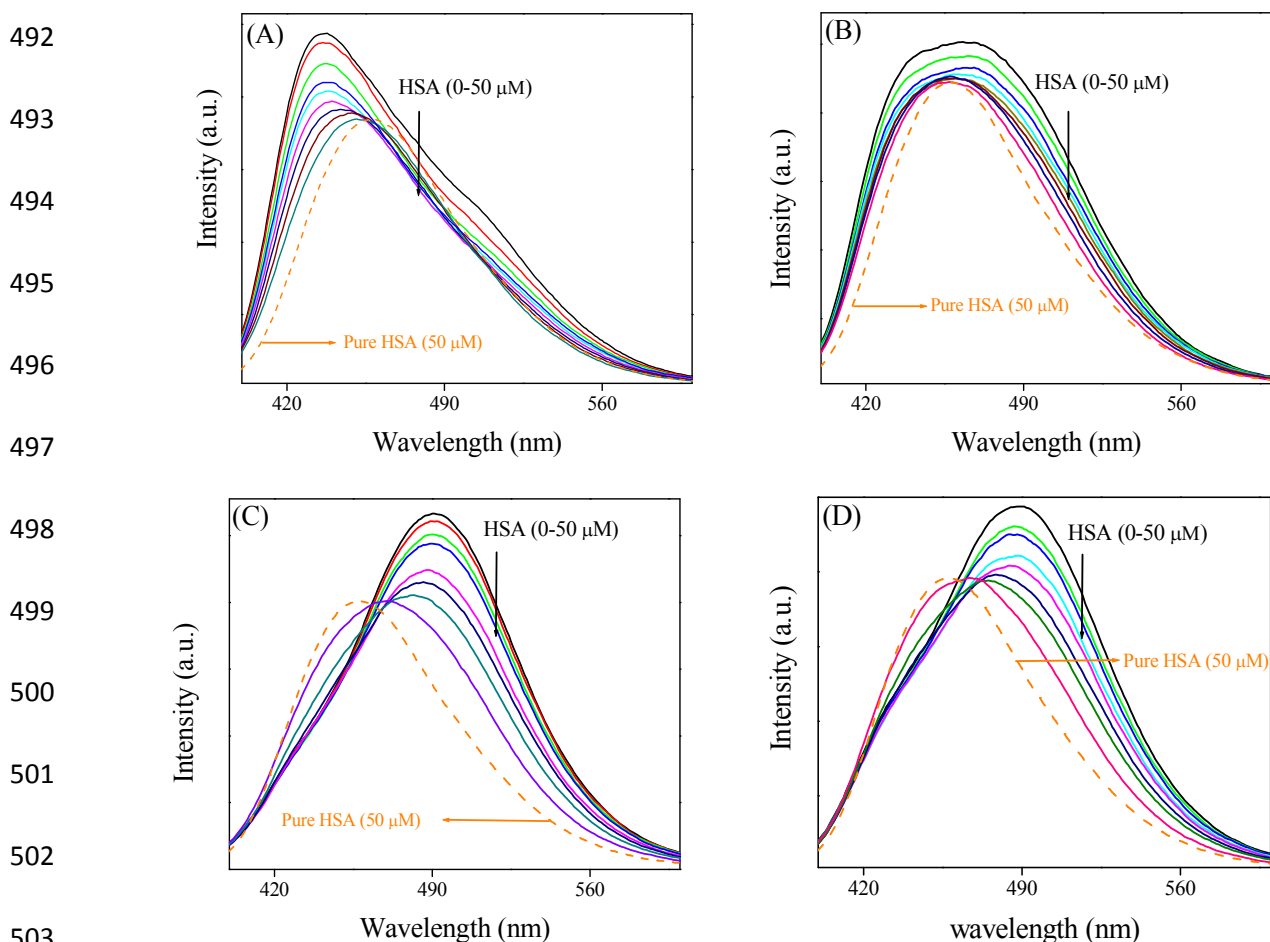
Figure 8. The steady state emission spectra of PRODAN in different liposomes as a function of
HSA concentration. (A) DPPC, (B) DMPC, (C) DOPC and (D) POPC. The dashed graph
represents emission spectra of PRODAN in native HSA which is normalized with respect to
highest concentration of HSA in liposomes.

508   There are two reasons that may be accounted for the observed quenching in liposomes. The first

509   one is the penetration of HSA into liposomes and the second is the release of PRODAN

510   molecules from liposome and subsequent migration to hydrophobic core of the HSA. Sabin and

511   co-workers[11a] reported that the forces which are involved in the interaction between liposomes

512   and HSA are of electrostatic and hydrophobic in nature. Primarily HSA interacts with the

513   liposome through electrostatic interaction to form HSA liposome complex and destabilize the

514   packing of lipid within bilayer and the order of acyl chain is reduced. The zeta potential (ξ) was

515   used to monitor the electrostatic interaction between liposomes and HSA.[11a] It was found that ξ

516   decreases exponentially with the protein concentration. The strong dependence of ξ was reported

517   as a patent evidence that the attractive electrostatic contribution has a major role in the formation

518   of liposome-HSA complex. A similar type of electrostatic interaction has been invoked by

519   Charbonneau and co-workers.[12] Sabin and co-workers[11a] also reported the protein penetration

520   inside the liposome. DSC measurement by them reveal that pretransition temperature of DMPC

521   liposomes decreases by more than one degree at the same time the enthalpy change (ΔH)

522   increases. A similar type of results were reported by Gatlantai and co-workers.[11b-c] The effect of

523   HSA over DMPC and DPPC liposomes indicates that protein penetrates into hydrophobic bilayer

524   affecting the packing of the hydrocarbon tails of lipids. Therefore, there is contribution of

525   hydrophobic forces in formation of liposome HSA-complexes. The contribution comes from

526   interaction between the lipid tails and parts of HSA that penetrate into the lipid bilayer. The

527   decrease in the interfacial tension indicates that protein molecules intercalate between the

528   hydrophobic tails of the lipid. This intercalation causes the leakage in the interfacial region

529   which facilitates the migration of the probe molecules from liposome to either aqueous phase or

530   hydrophobic pocket of HSA. Notably, upon addition of HSA to PRODAN impregnated

531   liposomes, the emission maxima are shifted towards the emission maximum of native HSA

532   (Figure 8). This observation led to the conclusion that PRODAN molecules being released from

533   the liposome are trapped in the hydrophobic pocket of HSA.

534   We compared the extent of quenching from Figure 9 in different liposomes by plotting ϕ_0/ϕ as a

535   function of concentration of HSA. Since we cannot calculate the local concentration of HSA, so;

536   we did not estimate Stern-Volmer quenching constant from this plot. It is observed from Figure 9

537   that among the un-conjugated lipids, quenching is higher in DPPC liposome compared to that in

538   DMPC liposomes. On the other hand in case of conjugated lipids, the quenching is little higher in

539   POPC liposomes compared to that in DOPC liposomes. The extent of quenching depends upon

540   the extent of perturbation of lipid bilayer by HSA. The significant difference in quenching in

541   DPPC and DMPC liposomes and little difference in DOPC and POPC liposomes may be

542   explained by considering the structural differences of different lipids, phase transition

543   temperature and prehydration level.

544

545

546

547

548

549
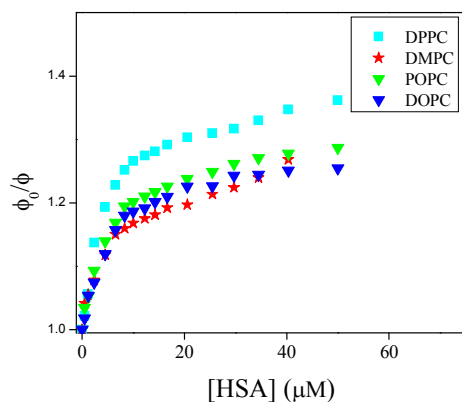
550   **Figure 9.** ϕ_0/ϕ Plot as a function of concentration of HSA (0-50 µM) in different liposomes.

551   In the present study, all the four lipids are zwitterionic and they possess similar head groups but

552   differ in their acyl chains. While DPPC and DMPC contain saturated acyl chain with different

553   chain length, POPC and DOPC contain unsaturated acyl chain with different number of carbon

554   atoms. As the length of hydrophobic acyl chain is the measure of hydrophobicity and it is already

555   reported that saturated fatty acids bind with greater affinity to albumins due to increase in

556   hydrophobic interaction,[39] in that sense the order of quenching follows the right trend. DPPC has

557   higher phase transition temperature than DMPC. The liposomes with lower phase transition

558   temperature remains more hydrated as compared to liposome with higher phase transition

559   temperature. Therefore DPPC is less hydrated as compared to DMPC. So; higher quenching is

560   observed in DPPC as compared to DMPC. Among POPC and DOPC bilayers, POPC is

561   monounsaturated while DOPC is bi-unsaturated with CH=CH in *cis* position. The unsaturated

562   fatty acids with a *cis* double bond, faces little steric restriction on binding to various sites on

563   protein.[40] Therefore perturbation of lipid bilayer by HSA will be more pronounced in POPC

564   bilayers as compared to DOPC bilayers. Along with this phase transition temperature of POPC is

565   higher than DOPC. The DOPC bilayers will remain in a more prehydrated state as compared to

566   POPC. Thus lower quenching is observed in DOPC as compared to POPC.

567   In this context the lifetime data may be helpful to unravel the dynamics of PRODAN inside the

568   liposome. We already mentioned that the fluorescence decay of PRODAN in aqueous buffer

569   solution is adequately fitted to a bi-exponential function with time constant 0.60 ns (74%) and

570   1.80 ns (26%). The lifetime of PRODAN is significantly enhanced when encapsulated in

571   liposomes. This is already discussed in the previous section. Table S_3A (in the supporting

572   information) reveals that PRODAN exhibits a tri-exponential decay with time components of

573   0.62 ns (15%), 2.73 ns (31%) and 6.57 ns (54%) in DPPC liposomes. We already assigned that

574   the picosecond component corresponds to the PRODAN molecules in the aqueous phase, 2.73 ns

575   component is attributed to the PRODAN molecules loosely bound in the interfacial region and

576   third component i.e. 6.57 ns component perhaps comes from those PRODAN molecules which

577   are strongly held inside the liposome. Addition of HSA to PRODAN impregnated DPPC

578   liposomes causes quenching in the lifetime components of PRODAN (Figure 10). After addition

579   of 2 μM HSA, the decays became bi-exponential and at 50 μM HSA the decay is comprised of

580   the components of 1.48 (40%) and 4.60 ns (60%). The significant quenching in the longer

581   component (from 6.48 ns to 4.60 ns) implies the penetration of HSA into liposome. The striking

582   observation is that the lifetime components of PRODAN in presence of 50 μM HSA in DPPC

583   liposomes (1.48 and 4.60 ns) are very similar to that in pure HSA (1.49 ns and 4.0 ns, Table S_1)

584   which indicates that PRODAN molecules upon interaction with HSA are released from liposome

585   and migrate to the hydrophobic pocket of HSA. Had the PRODAN molecules migrated to

586   aqueous phase, we would have obtained a picosecond component. We already mentioned that a

587   shift is observed in the steady state emission spectra of PRODAN upon addition of HSA which

588   indicates that PRODAN is migrating to the hydrophobic pocket of HSA. Thus this fact is

589   supported by the lifetime data.

590

591

592

593

594
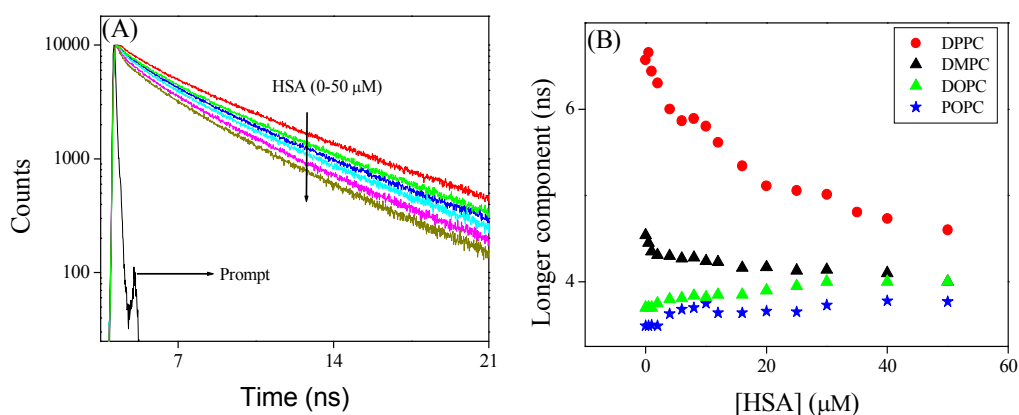
Figure 10. (A) Time resolved decays of PRODAN at different concentration of HSA in DPPC liposome. (B) Longer component of PRODAN in liposomes at different concentration of HSA.

However, a different result is obtained in DMPC-HSA system. It is revealed that unlike in DPPC system, DMPC offers only little decrement in lifetime components in presence of HSA. Addition of HSA causes a little quenching in the longer component from 4.55 to 4.10 ns while the shorter component decreases from 2.2 ns to 1 ns. The little quenching in the longer component indicates that, HSA has a less penetration in DMPC liposomes. The less penetration stems from the fact that DMPC because of its low phase transition temperature (23^0 C) remains nearly in liquid crystalline phase at room temperature and is much more hydrated than DPPC. As the hydrophobic interaction is responsible for the penetration of HSA into liposomes, therefore, HSA prefers DPPC over DMPC as former is more dehydrated hence is more hydrophobic compared to the latter. Although one should expect that DMPC is loosely packed and thus eases HSA to penetrate inside the liposome. However, higher quenching of the longer component in DPPC liposomes made it clear that hydrophobic interaction dominates over the other factors. On the other hand significant decrement in the shorter time component in DMPC liposomes indicates that HSA destabilize the interfacial region leaving the liposome core intact. Therefore, from the above results, we may conclude that the changes in the shorter component takes place when HSA destabilizes the interfacial region and the change in longer component in liposomes takes place when HSA affects the core of the liposomes due to penetration by hydrophobic interaction.[11a] The latter process depends on prehydration level of liposomes.

620   The above finding is again supported by the time resolved data in conjugated liposomes (Table

621   S_3B in the supporting information). In case of DOPC and POPC liposomes, we observe that the

622   lifetime of PRODAN is single exponential with a component around 3.49 ns and 3.77 ns

623   respectively. Addition of HSA results in quenching and time resolved decay becomes bi-

624   exponential. Surprisingly we observe a marginal increment in the longer component in POPC

625   (from 3.77 to 3.90 ns) and DOPC liposomes (3.40 to 3.77 ns). The observation in these two

626   liposomes clearly indicates the HSA does not penetrate in these two liposomes. On the other

627   hand appearance of picosecond component (0.86 to 0.95 ns) and increment in its amplitude up to

628   35-40% in both the liposomes indicates the leakage of PRODAN molecules and confirms the

629   fact that HSA destabilize the interfacial region of these liposome and core of the interfacial

630   region remains intact. It is noteworthy that in case of DPPC liposome similar kind of changes in

631   the population of shorter and longer components was observed. Therefore, it may unambiguously

632   be concluded that the leakage of PRODAN molecules takes place due to destabilization of

633   interfacial region of liposomes.

634   We carried out time resolved anisotropy measurements to probe interaction of liposomes with

635   HSA. The anisotropy decays are shown in Figure 11 and the results are summarized in Table 1.

636   PRODAN exhibits a single exponential decay with a time constant of 0.170 ns at 520 nm in

637   aqueous buffer solution at pH 7.40. In liposomes and liposomes-HSA complex the anisotropy

638   was measured at 450 nm. PRODAN exhibits bi-exponential anisotropy decays consisting of a

639   picosecond and a nanosecond component in all liposomes. The fast components (ϕ_{fast}) are around

640   0.47 (44%), 0.50 (45%), 0.40 (32%) and 0.416 ns (37%) in DPPC, DMPC, DOPC and POPC

641   liposomes respectively. On the other hand the slow components (ϕ_{slow}) are 2.77 (56%), 2.93

642   (55%), 2.25 (68%), and 2.20 ns (63%) in DPPC, DMPC, DOPC and POPC liposomes

643   respectively. It is revealed that addition of HSA to PRODAN loaded liposomes causes a

644   significant increment in ϕ_{slow}. Thus in presence 15 μM HSA, ϕ_{slow} were found to be 3.5 (60%),

645   3.90 ns (56%), 3.75 (40%), 3.60 (53%) in DPPC, DMPC, DOPC and POPC liposomes

646   respectively. Since liposomes and liposomes-HSA complex are big in the size, the motion of

647   liposome and liposome-HSA is too slow to impact on the overall rotational relaxation of

648   PRODAN. The increment in ϕ_{slow} may be due to the fact that the interfacial region of liposome

649   becomes compact due to electrostatic interaction between liposomes and HSA. It is revealed

25

650   from above mentioned result that the increment in ϕ_{slow} in DPPC and DMPC liposomes is less

651   compared to that in DOPC and POPC liposomes. The higher increment in ϕ_{slow} in DOPC and

652   POPC liposomes may be attributed to the fact that the interfacial region of DOPC and POPC

653   becomes more compact due to adsorption of HSA. The other explanation is that possibly lipid

654   packing order of DPPC and DMPC are much more affected by higher penetration of HSA in

655   these liposomes as compared to that in DOPC and POPC liposomes. This prevents the increment

656   in ϕ_{slow} in DPPC and DMPC liposomes. A similar conclusion was drawn in the discussion of

657   quenching in the time resolved data. Interestingly, we observed a decrement in the population of

658   ϕ_{slow} in case of DOPC and POPC liposomes. However, we do not observe any increment in the

659   population of slower component (β_{slow}). Since these two liposomes are soft in the interfacial

660   region, there is possibility that these two liposomes can accommodate more number of HSA

661   molecules which causes a significant leakage. Moreover, HSA penetrates deeper in DPPC and

662   DMPC liposomes, so; for these liposomes PRODAN can migrate to hydrophobic pocket of HSA.

663

664

669
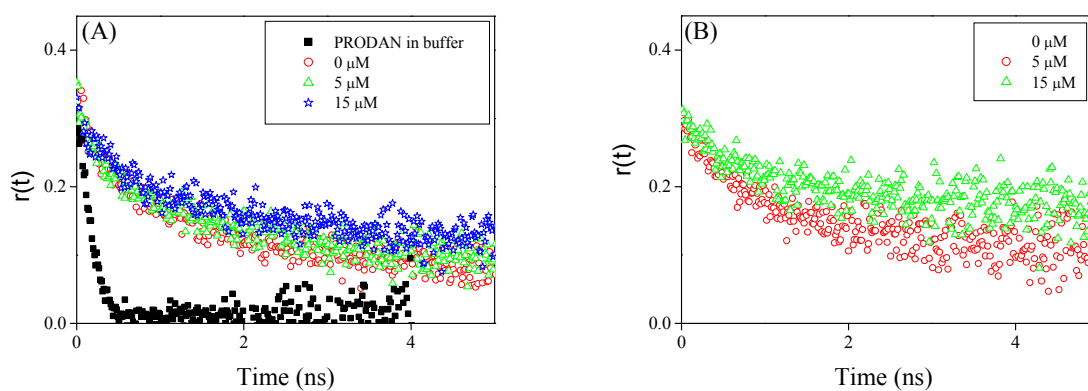
670   **Figure 11.** Fluorescence anisotropy decays of PRODAN at different concentration of HSA (A)

671   DMPC liposomes (B) DOPC liposomes.

672

673

674

26

675   **Table 1.** Rotational relaxation parameters of PRODAN in different liposomes and liposome-

676   HSA complex at $\lambda_{em} = 450$ nm[#]

677

System	$\beta_{fast}(\%)$	$\beta_{slow}(\%)$	φ_{fast} (ns)	φ_{slow} (ns)	r_0
PRODAN in Buffer solution, pH 7.4	1		0.17	-	0.29
DPPC	0.44	0.56	0.47	2.77	0.32
DPPC + 5 µM HSA	0.40	0.60	0.60	3.20	0.32
DPPC + 15 µM HSA	0.40	0.60	0.57	3.50	0.33
DMPC	0.45	0.55	0.50	2.93	0.35
DMPC + 5 µM HSA	0.42	0.58	0.39	3.46	0.35
DMPC + 15 µM HSA	0.45	0.55	0.37	3.90	0.33
DOPC	0.32	0.68	0.40	2.25	0.31
DOPC + 5 µM HSA	0.42	0.58	0.62	3.51	0.32
DOPC + 15 µM HSA	0.60	0.40	0.57	3.75	0.31
POPC	0.37	0.63	0.42	2.20	0.32
POPC + 5 µM HSA	0.39	0.61	0.45	2.99	0.33
POPC + 15 µM HSA	0.46	0.54	0.40	3.60	0.33

678

679   # The estimated error in the measurement is around 5%.

680

681

682

683

684

685 **Conclusion.** The present study reveals a clear understanding of how HSA interacts with

686 liposomes of saturated and unsaturated lipids having different phase transition temperature. The

687 CD measurement indicates that HSA is stabilized upon interaction with liposomes. Steady state

688 and time resolved fluorescence analysis reveal that HSA alters the packing order of liposome

689 through penetration and releases the encapsulated probe molecules from liposome, which

690 simultaneously migrates in the hydrophobic pocket of HSA. The penetration is apparently caused

691 by hydrophobic interaction between liposomes and HSA. The extent of penetration depends on

692 the prehydration level of liposomes. The liposomes of saturated lipids (DPPC and DMPC)

693 having higher phase transition temperature are less prehydrated at room temperature and hence

694 have stronger affinity towards HSA than that of liposomes of unsaturated lipids. The penetration

695 caused by hydrophobic interaction is revealed also in anisotropy measurement.

699

700

701

702

703

704

705

706

707

708

709

710 **References.**

711 1. L. J. Pike, *J. Lipid Res.,* 2003, **44**, 655.

712 2. (a) N. Ashgarian and Z. A. Schelly, *Biochim. Biopys. Acta,* 1999, **1418**, 295. (b) N. M.
713   Correa, Z. A. Schelly and H. Zhang, H. *J. Am. Chem. Soc.,* 2000, **122**, 6432.

714 3. T. Parassasi, G. D. Satasio, A. Ubaldo and E. Gratton, *Biophys J.,* 1990, **57**, 1179.

715 4. A. S. Klymchenko and A. P. Demchenko, *Langmuir,* 2002, **18**, 5637.

716 5. (a) A. Sytnik and I. Litvinyuk, *Proc. Natl. Acad. Sci. U.S.A.,* **1996**, 93, 12959. (b) S.
717   K. Sahoo and V. Labhasetwar, *Drug Discovery Today,* 2003, **8**, 1112.

718 6. A. Chonn, S. C. Semple and P. R. Cullis, *J. Biol. Chem.,*1992, **267**, 18759.

719 7. A. O. Pedersen, K. L. Mesenberg and U. Kragh-Hansen, *Eur. J. Biochem.,* 1995**, 233**, 395.

720 8. (a) S. Sugio, A. Kashima, S. Mochizuki, M. Noda and K. Kobayashi, *Protein Eng.*, 1999**,**
721   **12**, 439. (b) D. C. Carte and J. X. Ho, *AdV. Protein Chem.,* 1994, **45**, 153. (c) H. M. He
722   and D. C. Carter, *Nature,* 1992, **358**, 209. (d) T. Peters, *AdV. Protein Chem.,* 1985, **37**,
723   161. (e) S. Curry, P. Brick and N. P. Frank, *Biochim. Biophys. Acta,* 1999**, 1441**, 131.
724   (f) I. Petitpas, T. Grune, A. A. Battacharya and S. Curry, *J. Mol. Biol.,* 2001**, 314**, 955.
725   (g) E. L. Gelamo, C. H. T. P. Silva, H. Imasato and M. Tabak, *Biochim. Biophys. Acta,*
726   2002, **1594**, 84. (h) V. T. G. Chuang and M. Otagiri, *Biochim. Biophys. Acta,* 2001, **1546**,
727   337.

728 9. A. A. Bhattacharya, T. Grune and S. Curry, *J. Mol. Biol.,* 2000, **303**, 721.

729 10. (a) L. J. Lis, J. W. Kauffman and D. F. Shriver, *Biochim. Biophys. Acta,* 1976, **436**, 513.
730   (b) D. Hoekstra and G. Scherphoft, *Biochim. Biophys. Acta,* 1979**, 551**, 109.

731 11. (a) J. Sabin, G. Prieto, J. M. Ruso, P. V. Messina, F. J. Salgado, M. Nogueira, M. Costas
732   and F. I. Sarmiento, *J. Phys. Chem. B,* 2009, **113**, 1655. (b) R. Galantai and I. Ba´rdos-
733   Nagy, *Int. J. Pharm.,* 2000, **195**, 207. (c) I. Ba´rdos-Nagy, R. Galantai, M. Laberg and J.
734   Fidy, *Langmuir,* 2013**, 19,**146.

735 12. D. Charbonneau, M. Beauregard and H. A. Tajmir-Riahi, *J. Phys. Chem. B,* 2009, **113,**
736   1777.

737 13. (a) L. P. Tseng, H. J. Liang, T. W. Chung, Y. Y. Huang and D. Z. Liu, *J. Med.& Biol.*
738   *Engg.,* 2007, **27,** 29. (b) C. K. Kim and D. K. Park, *Arch. Pharm. Res.,* 1987, **10**, 75. (c) J.
739   Hernandez, J. Estelrich, M. T. Montero and O. Valls, *Int. J. Pharm.,* 1989**, 57,** 211. (d) T.
740   P. W. McMullen and R. N. McElhaney, *Curr. Opin. Coll. Interf. Sci.,* 1996**, 1**, 83.

741   14. D. E. Vance, and J. E. Vance, *Biochemistry of lipids, Lipoproteins and membranes*;
742   Elsevier Science: Vancouver, B. C. Canada, **1995**.

743   15. A. L. Arbuzova and R. E. Koeppe, *Annu. Rev. Biophys. Biomol. Struct.,* 2007, **37***,* 107.

744   16. D. L. Nelson and M. M. Cox, *Principles of Biochemistry,* 4th Ed.*,* W. H. Freeman and
745   company, U. S. A, New York, **2008.**

746   17. R. Thakur, A. Das and A. Chakraborty, *Phy. Chem. Chem. Phys.,* 2012**, 14***,* 15369.

747   18. J. R. Lakowicz, *Principles of Fluorescence Spectroscopy,* 3rd Ed., Kluwer Academic
748   Plenum Publisher, New York , **2006.**

749   19. (a) A. B. J. Parusel, *J. Chem. Soc., Faraday Trans*., 1998, **94**, 2923. (b) A. B. J.
750   Parusel, W. Nowak and S. Grimme, *J. Phys. Chem. A,* 1998 , **102***,* 7149. (c) W.
751   Nowak, P. Adamczak, A. Balter and A. Sygula, *J. Mol. Struct. THEOCHEM,* 1986,
752   **32**, 13. (d) A. I. Harianawala and R. H. Bogner, *J. Lumin.,* 1998, **79***,* 97. (e) D. Marks,
753   P. Prosposito, H. Zhang and M. Glasbeek, *Chem. Phys. Lett.,* 1998, **289**, 535.

754   20. (a) S. Guha, K. Sahu, D. Roy, S. K. Mondal, S. Roy and K. Bhattacharyya,
755   *Biochemistry*, 2005, **44**, 8940. (b) E. K. Krasnowska, L. A. Bagatolli, E. Gratton and
756   T. Parasassi, *Biochem. Biophys. Acta,* 2001, **1151**, 330. (c) N. A. Pasdar and E. C. Y.
757   L. Chan, *Food Hydrocoll.,* 2001, **15***,* 285. (c) O. P. Bondar and E. S. Rowe, *Biophys.*
758   *J.,* 1999, **76**, 956.

759   21. (a) R. B. Macgregor and G. Weber, *Nature,* 1986**, 319***,* 70. (b) A. Balter, W. Nowak
760   and W. Pawelkiewicz, *Chem. Phys. Lett.,* 1988, **143***,* 565.

761   22. (a) C. E. Bunker, T. L. Bowen and Y. P. Sun, *Photochem. Photobiol.,* 1993, **58**, 499.
762   (b) A. Samanta and R. W. Fessenden, *J. Phys. Chem. A,* 2000, **104**, 8972.

763   23. (a) S. K. Pal, D. Mandal and K. Bhattacharyya, *J. Phys. Chem. B,* 1998, **102**, 11017.
764   (b) B. C. Lobo and C. J. Abelt, *J. Phys. Chem. A,* 2003, **107**, 10938. (c) B. Mennucci,
765   M. Caricato, F. Ingrosso, C. Cappelli, R. Cammi, J. Tomasi, G. Scalmani and M. J.
766   Frisch, *J. Phys. Chem. B,* 2008, **112**, 414. (c) M. Brozis, V. I. Tomin and J. Heldt, *Zh*
767   *Prikl Spectrosk* **2002,** *69,* 589.

768   24. (a) H. Rottenberg, *Biochemistry,* 1992, **31***,* 9473. (b) O. P. Bondar and E. S. Rowe,
769   *Biophys. J.,* 1999, **71***,* 1440. (c) A. Sommer, F. Paltauf and A. Hermetter,
770   *Biochemistry,* 1990, **29***,* 11134. (d) E. K. Krasnowska, E. Gratton and T. Parasassi,

Biophys. J., 1998, **74***,* 1984. (e) J. Zeng and P. L. G. Chong, *Biochemistry,* 1991, **30***,* 9485.

25. (a) B. Sengupta, J. Guharay and P. K. Sengupta, *Spectrochemica Acta Part A* 2000, **56***,* 1433. (b) F. M. Agazzi, J. Rodriguez, R. D. Falcone, J. J. Silber and N. M. Correa, *Langmuir,* 2013**, 29***,*3556. (c) M. Novaira, F. Moyano, M. A Biasutti, J. J Silber and N. M. Correa, *Langmuir* 2008**, 24***,* 4637. (d) M. Novaira, M. A. Biasutti, J. J. Silber and N. M. Correa, *J. Phys. Chem. B* **2007, 111***,* 748. (e) S. S. Quintana, R. D. Falcone, J. J. Silber and N. M. Correa, *ChemPhysChem* **2012, 13***,* 115. (f) A. M. Durantini, R. D. Falcone, J. J. Silber and N. M. Correa, *ChemPhysChem* 2009**, 10***,* 2034. (g) R. Adhikary, C. A. Barnes and J. W. Petrich, *J. Phys. Chem. B* 2009, **113**, 11999.

26. (a) P. L. G. Chong, *Biochemistry,* 1988, **27***,* 399. (b) C. C. de Vequi- Suplicy and C. R. Benatti and M. T. Lamy, *J. Fluoresc.,* 2006**, 16***,* 365.

27. (a) J. Sy´kora, P. Kapusta, V. Fidler and M. Hof, *Langmuir*, 2002, **18***,* 571. (b) P. Jurkiewicz, A. Olzùyn´ska, M. Langner and M. Hof, *Langmuir,* 2006**, 22**, 8741. (c) L. Cwiklik, A. J. A. Aquino, M. Vazdar, P. Jurkiewicz, J. Pittner, M. Hof and H. Lischka, *J. Phys. Chem. A,* 2011, **115**, 11428.

28. (a) T. Parasassi, G. De Stasio, A. Ubaldo and E. Gratton, *Biophys. J.,* 1990*,* **57***,* 179. (b) T. Parasassi, E. K. Krasnowska, L. Bagatolli and E. Gratton, *J. Fluorescence,* 1998, **8***,* 365.

29. (a) S. S. Krishnakumar and D. Panda, *Biochemistry,* 2002*,* **41***,* 7443. (b) S. Basak, D. Debnath, H. Haque, S. Ray and A. Chakrabarti, *Ind J. Biochem and Biophys.,* 2001, **38***,* 84. (c) P. Abbyad, X. Schi, W. Childs, T. B. McAnaney, B. E. Cohen and S. G. Boxer, *J. Phys. Chem. B,* 2007, **111***,* 8269. (d) A. Chakrabarti, *Biochem. Biophys. Res.Com.,* 1996, **226**, 495. (e) A. Chakrabarti, D. A. Kelkar, A, Chattopadhyay, *Biosci Rep.,* 2006*,* **26**, 386 (f) A. Chattopadhyay, S. S. Rawat, D. A. Kelkar, S. Ray, A. Chakrabarti, *Protein Science* 2003, **12**, 2403.

30. (a) D. Zhong, A. Douhal and A. H. Zewail, *Proc. Natl. Acad. Sci. U. S. A.,* 2000, **97***,* 14056. (b) J. K. A. Kamal, L. Zhao and A. H. Zewail, *Proc. Natl. Acad. Sci. U. S. A.,* 2004**, 101***,*13411.

800   31. a) D. C. Carter, J. X. Ho, *Adv. Protein Chem.,* **1994**, **45***,* 152. (b) T. Peters, Jr. *All about*
801   *Albumins: Biochemistry, Genetics, and Medical Applications;* Academic Press: San
802   Diego, **1996.**
803   32. (a) B. Farruggia, F. Garcia and G. Pico´, *Biochim. Biophys. Acta,* 1995**, 1252**, 59. (b)
804   B. Nerli, D. Romanini and G. Pico´, *Chem. Biol. Interact.,* 1997**, 104**, 179.
805   33. F. Moreno, M. Cortijo and J. G. Jimenez, *Photochem. Photobiol.,* 1999, **69**, 8.
806   34. R. Thakur, A. Mallik and A. Chakraborty, *Photochem.& Photobiol.,* 2012**, 88***,* 1248.
807   35. F. Moyano, M. A. Biasutti, J. J. Silber and N. M. Correa, *J. Phys. Chem. B,* 2006**, 110***,*
808   11838.
809   36. B. A. C. Horta, A. H. de Vries and P. H. Heunenberger, *J. Chem. Theory Comput.,* 2010,
810   **6**, 2488.
811   37. Z. Huang and R. P. Haugland, *Biochem. Biophys. Res. Commun*., 1991, **181**, 166
812   38. (a) A. Gerbanowski, C. Malabat, C. Rabiller and J. Gueguen, *J. Agric. Food Chem. ,* 1999,
813   **47***,* 5218. (b) Y. Moriyama and K. Takeda, *Langmuir,* 1999, **15**, 2003.
814   39. A. A. Spector, *J. Lipid Res.,* **1975,** *16,* 165.
815   40. (a) V. G. Richieri, A. Anel and M. K. Alan, *Biochemistry,* 1993**, 32***,* 7574.
816   (b) D. P. Cistola, D. M. Small and J. A. Hamilton, *The J. Biol Chem.,* 1987**, 262***,* 10971.
817   (c) J. S. Parks, D. P. Cistola, D. M. Small and J. A. Hamilton, *The J. Biol Chem.,* 1983,
818   **258**, 9262.
819
820
821
822
823
824
825
826
827